

SCALE ANALYSIS OF DECAY HEAT REMOVAL SYSTEM BETWEEN HTR-10 AND HTR-PM REACTORS UNDER ACCIDENTAL CONDITIONS

Thiago D. Roberto¹, Celso M. F. Lapa², and Antonio C. M. Alvim³

¹Programa de Engenharia Nuclear (PEN/ COPPE/UFRJ - RJ)
Cidade universitária, Centro de Tecnologia, bloco G, sala G-206, Ilha do Fundão
21941-972 Rio de Janeiro, RJ
thiagodbr@gmail.com

²Instituto de Engenharia Nuclear (IEN / CNEN - RJ)
Rua Hélio de Almeida, 75
Cidade Universitária, Ilha do Fundão
21941-972 Rio de Janeiro, RJ
lapa@ien.gov.br

³Programa de Engenharia Nuclear (PEN/ COPPE/UFRJ - RJ)
Cidade universitária, Centro de Tecnologia, bloco G, sala G-206, Ilha do Fundão
21941-972 Rio de Janeiro, RJ
alvim@nuclear.ufrj.br

ABSTRACT

The 10 MW high-temperature gas-cooled test module (HTR-10) is a graphite-moderated and helium-cooled pebble bed reactor prototype that was designed to demonstrate the technical and safety feasibility of this type of reactor project under normal and accidental conditions. In addition, one of the systems responsible for ensuring the safe operation of this type of reactor is the passive decay heat removal system (DHRS), which operates using passive heat removal processes. A demonstration of the heat removal capacity of the DHRS under accidental conditions was analyzed based on a benchmark problem for design-based accidents on an HTR-10, i.e., the pressurized loss of forced cooling (PLOFC) described in technical reports produced by the International Atomic Energy Agency. In fact, the HTR-10 is also a proof-of-concept reactor for the high-temperature gas-cooled reactor pebble-bed module (HTR-PM), which generates approximately 25 times more heat than the HTR-10, with a thermal power of 250 MW, thereby requiring a DHRS with a higher system capacity. Thus, because an HTR-10 is a prototype reactor for an HTR-PM, a scaling analysis of the heat transfer process from the reactor to the DHRS was carried out between the HTR-10 and HTR-PM systems to verify the distortions of scale and the differences between the main dimensionless numbers from the two projects.

1. INTRODUCTION

Nuclear power plants (NPPs) contribute significantly to clean energy generation, and thus significantly reduce the environmental impact of electricity generation. The benefits of nuclear energy are many, and can even extend to other energy products besides electricity, such as the generation of hydrogen. These new nuclear energy systems are known as generation IV

reactors, and are characterized by improved sustainability, economics, safety, proliferation resistance, and physical protection.

One of these new nuclear power systems is the VHTR, which is a graphite-moderated, helium-cooled reactor with a thermal neutron spectrum. It can supply nuclear heat and electricity over a range of core outlet temperatures between 700°C and 950°C, and in the future, it is expected to operate at core outlet temperatures higher than 1000°C. The reactor core type of the VHTR can be a prismatic block core such as the Japanese high-temperature test reactor (HTTR) or a pebble-bed core such as the Chinese 10 MW high-temperature gas-cooled test module reactor (HTR-10) [4].

Two Chinese reactor projects are analyzed in this work, the HTR-10 and the high-temperature gas-cooled reactor pebble-bed module (HTR-PM). Both reactors are the pebble-bed core type, with the HTR-10 being a proof of concept for the HTR-PM. The reactors share several project similarities, including a reactor cavity that needs to be cooled using a reactor cavity cooling system (RCCS). With the goal of verifying the inherent safety of these systems, a similarity analysis of the RCCS between the two reactors based on the benchmark problem of a pressurized loss of forced cooling was conducted.

2. THEORY

2.1. High-temperature gas-cooled reactor under development in China

2.1.1. HTR-10

The pebble-bed HTR-10 reactor is located at the Nuclear Energy Institute of Technology (INET) at Tsinghua University, Beijing. This reactor reached its first criticality using air in December 2000, and reached its full potential of 10 MW of thermal energy for 72 h in February 2003 [5].

The HTR-10 is a helium-cooled graphite-moderated reactor with a thermal neutron spectrum. Its primary system operates at 3 MPa, with core inlet and outlet temperatures of 250°C and 700°C, respectively, although the main focus of the VHTR is a high temperature of approximately 1000°C. That has been imposed because of the technical risks associated with high temperatures, and because the HTR-10 is a test reactor designed with the following primary objectives [9]:

- to acquire the know-how to design, construct, and operate an operate high-temperature gas-cooled reactor HTGRs,
- to demonstrate the inherent safety features of a modular HTGR;
- to establish an irradiation and experimental facility for fuel elements and materials; and
- to carry out R&D for nuclear high-temperature process-heat applications.

The reactor primary system is shown in Figure 1, which was adapted from [1].

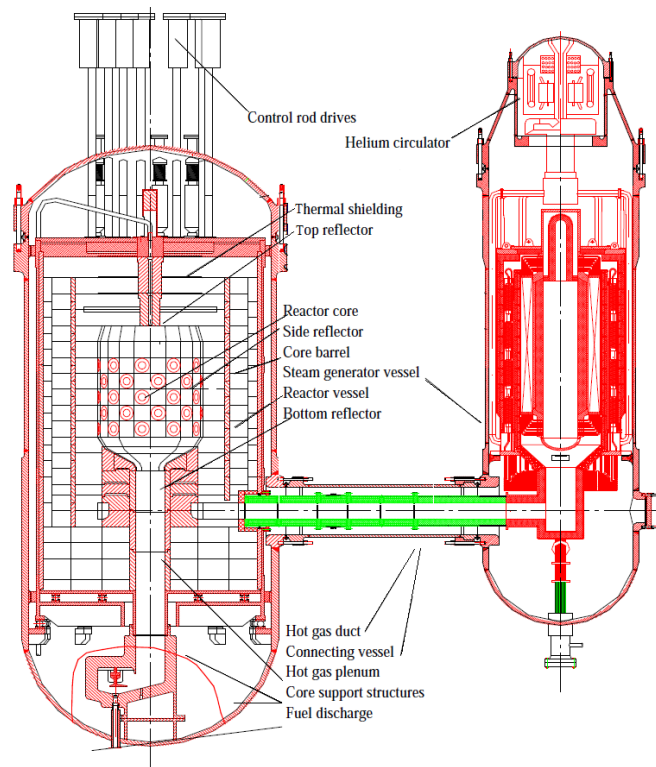


Figure 1: HTR-10 primary system.

2.1.2. High-Temperature gas-cooled Reactor-Pebble bed Module (HTR-PM)

An HTR-PM unit is under construction at Shidaowan in China's Shandong province. The China Huaneng Group (CHNG) is the leading organization in the consortium building the Shidaowan HTR-PM demonstration plant, along with the China Nuclear Engineering & Construction Group (CNEC) and Tsinghua University's INET, which is an R&D leader [6].

The HTR-PM is a 458 MW thermal power helium-cooled graphite-moderated reactor with a thermal neutron spectrum. Its primary system operates at 7 MPa, with core inlet and outlet temperatures of 250°C and 750°C, respectively [8].

According to [7], the major objectives of the HTR-PM can be summarized as follows:

- Completing a 200 MWe HTR-PM demonstration plant, and providing a sound foundation for the further development of a generation IV nuclear system.

Its technical objectives are as follows:

- demonstration of inherent safety features;
- demonstration of cost competitiveness;
- standardization and modularization; and
- confirmation of proven technologies.

The primary system of the reactor is shown in Figure 2, which was adapted from [8].

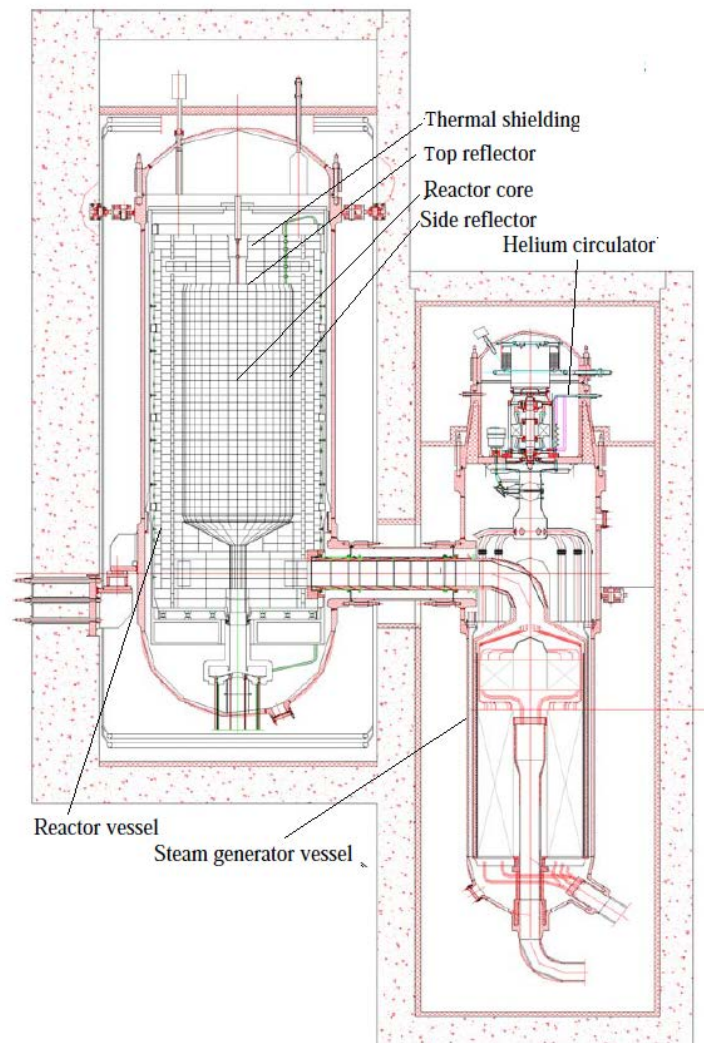


Figure 2: HTR-PM primary system.

2.2. Passive decay heat removal system

In both projects, the entire primary system is confined by the containment. The containment includes the reactor cavity, the steam generator cavity, and the discharge system of the fuel elements cavity. Reactor cavity cooling system (RCCS) is required to protect the concrete structures of the containment from high temperatures originating from the reactor pressure vessel (RPV) (The RCCS is one of the systems of passive decay heat removal systems). Thus, the RCCS was conceived during the project, as shown in Figure 3, which was adapted from [2].

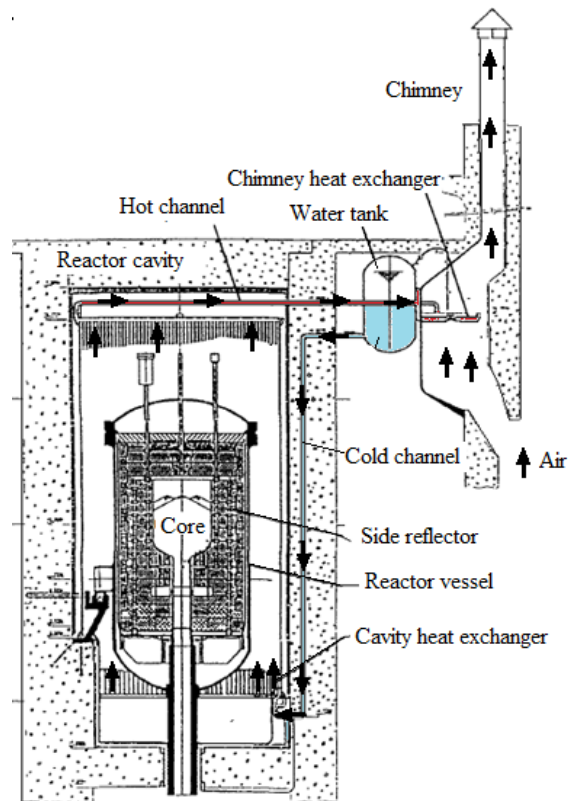


Figure 3: HTR-10 Reactor cavity cooling system.

The RCCS consists mainly of heat exchangers inside the reactor cavity and air coolers in the chimney, thereby generating a natural-circulation circuit. This system is also applied during an accident. For example, during a normal reactor shutdown process, the helium circulator and steam generator act together to remove residual heat from the core. However, if this system fails, residual heat can be removed passively through the RCCS system.

It was assumed that the RCCS structure of the HTR-PM is similar to that of the HTR-10. The necessary parameters for a similarity analysis of the system used in both reactors were extracted from a benchmark analysis. In a pressurized loss of forced cooling accident (PLOFC) analysis, the following conditions were assumed:

- the forced circulation of the coolant is stopped;
- the reactor undergoes a scram;
- the working pressure is sustained;
- natural convection of the helium occurs in the core;
- the RPV temperatures are assumed to be constant;
- the pressure of the reactor cavity is assumed to be 1 atm; and
- the panel RCCS temperatures are assumed to be constant.

The analysis is conducted on the components inside the reactor cavity, RPV, and RCCS standpipes, whereas the other components outside the reactor cavity are simply neglected.

3. METHODOLOGY

3.1. Conservation equations

3.1.1. Cavity region similarity

Owing to the symmetry of the RCCS cavity, it is possible to apply an approximation to a rectangular two-dimensional cavity with the two horizontal walls being isolated, one of the vertical walls being heated (reactor pressure vessel), and the other wall being cooled (the RCCS standpipes). Considering a steady-state condition, the equations for mass, momentum, and energy conservation can be written as follows:

$$\frac{\partial v_x}{\partial x} + \frac{\partial v_y}{\partial y} = 0, \quad (1)$$

$$\rho C_p \left(v_x \frac{\partial T}{\partial x} + v_y \frac{\partial T}{\partial y} \right) = k \left(\frac{\partial^2 T}{\partial x^2} + \frac{\partial^2 T}{\partial y^2} \right), \quad (2)$$

$$\rho \left(v_x \frac{\partial v_y}{\partial x} + v_y \frac{\partial v_y}{\partial y} \right) = -\rho g - \frac{\partial P}{\partial y} + \mu \left(\frac{\partial^2 v_y}{\partial x^2} + \frac{\partial^2 v_y}{\partial y^2} \right), \quad (3)$$

$$\rho C_p \left(v_x \frac{\partial T}{\partial x} + v_y \frac{\partial T}{\partial y} \right) = k \left(\frac{\partial^2 T}{\partial x^2} + \frac{\partial^2 T}{\partial y^2} \right), \quad (4)$$

where P is the pressure; V_x and V_y are the velocity component in the horizontal and vertical directions, respectively; k is the thermal conductivity; C_p is the specific heat; and g is the gravity.

The following non-dimensional variables are defined:

$$y^* = \frac{y}{H_{cav}}, x^* = \frac{x}{H_{cav}}, V_x^* = \frac{V_x}{V_{Re}}, V_y^* = \frac{V_y}{V_{Re}}, P^* = \frac{P + \rho_0 g y}{\rho V_{Re}^2}, \Theta^* = \frac{T - T_0}{T_{sR} - T_{sS}}, \quad (5)$$

where H_{cav} is the cavity height; Θ^* is the non-dimensional temperature; V_{Re} is the reference velocity in the air-cavity region; T_{sR} and T_{sS} are the average temperature of the RPV wall and the external wall of the standpipes, respectively; and ρ_0 is the density at the reference temperature, T_0 . The superscript $*$ indicates a dimensionless variable.

A Boussinesq approximation can be used to link the change in temperature to the change in density on the right side of equation (3). Thus, using equations (5), equations (1)–(4) can be written in non-dimensional form as

$$\frac{\partial v_x^*}{\partial x^*} + \frac{\partial v_y^*}{\partial y^*} = 0, \quad (6)$$

$$v_x^* \frac{\partial v_x^*}{\partial x^*} + v_y^* \frac{\partial v_x^*}{\partial y^*} = -\frac{\partial p^*}{\partial x^*} + \frac{1}{\text{Re}} \left(\frac{\partial^2 v_x^*}{\partial x^{*2}} + \frac{\partial^2 v_x^*}{\partial y^{*2}} \right), \quad (7)$$

$$v_x^* \frac{\partial v_y^*}{\partial x^*} + v_y^* \frac{\partial v_y^*}{\partial y^*} = -\frac{\partial p^*}{\partial y^*} + \frac{G_r}{\text{Re}^2} \Theta^* + \frac{1}{\text{Re}} \left(\frac{\partial^2 v_y^*}{\partial x^{*2}} + \frac{\partial^2 v_y^*}{\partial y^{*2}} \right), \quad (8)$$

$$v_x^* \frac{\partial \Theta^*}{\partial x^*} + v_y^* \frac{\partial \Theta^*}{\partial y^*} = \frac{1}{\text{Pe}} \left(\frac{\partial^2 \Theta^*}{\partial x^{*2}} + \frac{\partial^2 \Theta^*}{\partial y^{*2}} \right), \quad (9)$$

where Re is the Reynolds number, which is defined as

$$\text{Re} = \frac{\rho V_{\text{Re}} H_{\text{cav}}}{\mu}, \quad (10)$$

where μ is the dynamic viscosity.

The Pe number is given based on the product of the values of Re and Pr, and can be written as

$$\text{Pe} = \text{Re} \times \text{Pr} = \frac{\rho V_{\text{Re}} H_{\text{cav}} C_p}{k}. \quad (11)$$

The reference velocity is taken when the Re is normalized to unity, and thus, the reference velocity can be defined as

$$V_{\text{Re}} = \frac{\mu}{\rho H_{\text{cav}}}. \quad (12)$$

The Grashof number (Gr) can be defined as

$$\text{Gr} = \frac{g \rho \beta (T_{\text{sR}} - T_{\text{SS}}) H_{\text{cav}}^3}{\mu^2}, \quad (13)$$

where β is the isobaric thermal expansion coefficient.

The definition of the reference velocity for the cavity implies that the inertia forces are of the same order of magnitude as the viscous forces. Thus, the Grashof number provides the ratio of buoyancy forces over viscous forces, where the buoyancy forces are the driving phenomenon, and the viscous forces are the dissipative phenomenon.

Here, Gr/Re^2 is the relationship between the buoyancy and inertia forces and can be defined as follows:

$$\frac{\text{Gr}}{\text{Re}^2} = \frac{g \beta (T_{\text{sR}} - T_{\text{SS}}) H_{\text{cav}}}{V_{\text{Re}}^2}. \quad (14)$$

The ratio Gr/Re^2 can be used to determine the flow regime. If $\text{Gr}/\text{Re}^2 \gg 1$, then the buoyancy forces prevail over the inertia forces, i.e., natural convection occurs. If $\text{Gr}/\text{Re}^2 \ll 1$, then the

inertia forces prevail over the buoyancy forces, i.e., forced convection occurs. In the case of $Gr/Re^2 \approx 1$, mixed convection occurs.

3.1.2. Similarity of RCCS standpipes

The RCCS analysis was conducted only under steady-state conditions. The one-dimensional and simplified momentum and energy equations were applied to the RCCS standpipes inside the reactor cavity. The simplified system is shown in Figure 4.

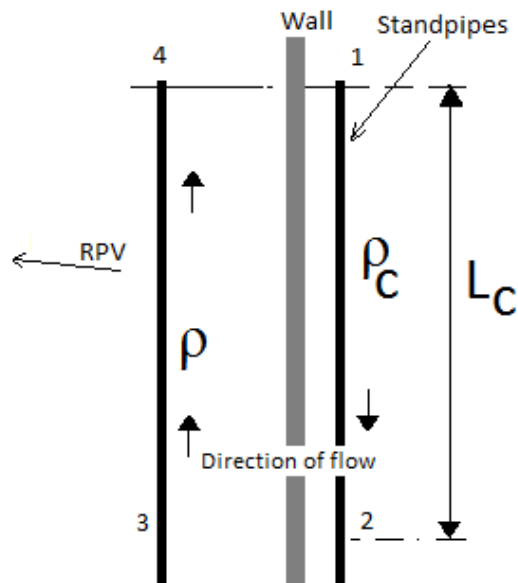


Figure 4: Simplified RCCS system inside the reactor cavity.

The integral momentum equation in the standpipes side of the RCCS can be written as

$$P_1 + \rho_c g l_c = P_4 + \int_0^{l_c} \rho g dy + \delta p_{\text{friction}} + \delta p_{\text{form}}, \quad (15)$$

where the loss of pressure terms in section i are defined as follows.

$$\delta p_{\text{friction}} = \sum_i \frac{1}{2D_i} f_i \rho_i V_i^2 l_i \quad (16)$$

$$\delta p_{\text{form}} = \sum_i \frac{1}{2} K_i \rho_i V_i^2 \quad (17)$$

Here, l_c is the length of the heated section of the standpipes, D is the hydraulic diameter, K is the localized pressure loss coefficient, f is the friction factor, l is the length, and v is the velocity.

The following non-dimensional variables are defined:

$$y^* = \frac{y}{H_{cav}}, V_i^* = \frac{V_i}{V_e}, l_c^* = \frac{l_c}{H_{cav}}, \Theta^* = \frac{T - T_{in}}{T_{out} - T_{in}}, \Delta P^* = \frac{\Delta P}{\rho_e V_e}. \quad (18)$$

The velocity in section I can be defined based on the continuity equation as

$$V_i = V_e \left(\frac{A_e}{A_i} \right), \quad (19)$$

where V_e is the water velocity at the inlet of the standpipes; T_{in} and T_{out} are the reference temperatures at the inlet and outlet of the standpipes, respectively; A_e is the total cross flow area of the standpipes; and ρ_e is the reference water density at the inlet of the standpipes.

The Boussinesq approximation can be used to link the change in temperature to the change in density on the right side of equation (15). Thus, using equations (18) and (19), equations (15)–(17) can be written in non-dimensional form as

$$\Delta P^* + R_i \left[-\Theta_c^* l_c^* + \int_0^{l_c^*} \Theta^* dy^* \right] - \frac{1}{2} V_e^2 \left[\sum_i \left(\frac{f_i l_i}{D_i} + K_i \right) \left(\frac{A_e}{A_i} \right)^2 \right] = 0, \quad (20)$$

where R_i is the Richardson number and is defined as

$$R_i = \frac{g H_{cav} \beta (T_{out} - T_{in})}{V_e^2}. \quad (21)$$

The energy equation for the fluid in the inner pipe is

$$\frac{\pi}{4} D_i^2 V_i \rho C_p \frac{\partial T}{\partial y} = \pi D_i^2 h_{cond} (T_{SS} - T_{IS}), \quad (22)$$

where D_i is the internal diameter of the standpipe of the RCCS; V is the velocity of the water inside the standpipe; T is the temperature of the fluid inside the standpipe; h_{cond} is the heat exchange coefficient through the conduction of the fluid; and T_{SS} and T_{IS} are the external and internal temperatures of the RCCS standpipes, respectively.

The heat exchange coefficient at the wall of the circular tubes is given based on the definition of the Nusselt number and the Dittus-Boelter correlation as

$$h_{cond} = \frac{k}{D_h} 0.023 \left(\frac{\rho V_e D_h}{\mu} \right)^{0.8} \left(\frac{\mu C_p}{k} \right)^{0.4}, \quad (23)$$

where k is the thermal conductivity; and D_h is the hydraulic diameter of the standpipe.

Using the variables defined in equations (18) and the continuity equation defined through equation (19), the energy equation can be rewritten in a dimensionless form as

$$V_e \frac{A_e}{A_i} \frac{\partial \Theta}{\partial y^*} = S_t (\Theta_{ss}^* - \Theta_{is}^*), \quad (24)$$

where S_t is the Stanton number, which is defined as

$$S_t = \frac{4h_{\text{cond}}H_{\text{cav}}}{D_i C_p \rho V^*}. \quad (25)$$

The heat transferred from the RPV to the RCCS can be written approximately as

$$Q(t) = A_c h_{\text{cav}} (T_{sR} - T_{sS}) + A_{\text{rad}} \varepsilon \sigma (T_{sR}^4 - T_{sS}^4), \quad (26)$$

where A_c is the total external area of the standpipe, A_{rad} is the outer area of the standpipe facing the reactor, h_{cav} is the heat exchange coefficient for the air-cavity region, ε is the emissivity, and σ is the Stefan-Boltzmann constant.

In estimating the heat transferred during natural convection, the heat exchange coefficient h_{cav} is calculated from the Nusselt number Nu , which can be calculated through the following formula:

$$Nu = 0.096(Gr \times Pr)^{0.306}, \quad (27)$$

at steady-state conditions:

$$Q_0 = A_e V_e \rho_e c_p (T_{\text{out}} - T_{\text{in}}). \quad (28)$$

The ratio of equation (26) to equation (28) gives us the following dimensionless equation:

$$Q^* = \frac{Q(t)}{Q_0} = N_c (\Theta_{sR}^* - \Theta_{sS}^*) + N_{\text{rad}} \{ [\Theta_{sR}^* N_T + 1]^4 - [\Theta_{sS}^* N_T + 1]^4 \}, \quad (29)$$

where dimensionless numbers can be defined as

$$N_c = \frac{A_c h_{\text{cav}}}{A_e V_e \rho_e c_p}, \quad (30)$$

$$N_{\text{rad}} = \frac{A_{\text{rad}} \varepsilon \sigma T_{\text{in}}^4}{A_e V_e \rho_e c_p (T_{\text{out}} - T_{\text{in}})}, \quad (31)$$

$$N_T = \frac{T_{\text{out}}}{T_{\text{in}}} - 1, \quad (32)$$

where N_c is the dimensionless number of conduction, and represents the relation between the heat transferred from the RPV to the standpipes through convection and the total amount of heat transferred, N_{rad} is the dimensionless amount of radiation and represents the ratio of the

heat transferred from the RPV to the N_T is a dimensionless number indicating the temperature ratios.

Using the approximation of equation (28), it is possible to rewrite the equations for the Richardson number, the cavity radiation number, and the temperature ratio number:

$$(T_{out} - T_{in}) = \frac{Q_0}{A_e V_e \rho_0 c_p}, \quad (33)$$

$$R_i = \frac{g H_{cav} \beta Q_0}{A_e \rho_0 c_p V_e^3}, \quad (34)$$

$$N_{rad} = \frac{A_{rad} \varepsilon \sigma T_{in}^4}{Q_0}, \quad (35)$$

$$N_T = \frac{Q_0}{T_{in} A_e V_e \rho_0 c_p}. \quad (36)$$

3.2. Scaling Analysis of the RCCS

The objective of the scaling procedure is to verify the RCCS similarity between the HTR-10 and HTR-PM in the benchmark problem mentioned above, which means verifying the ratio of the similarity group of the HTR-10 (Π_{HTR-10}) to that of the HTR-PM (Π_{HTR-PM}) as

$$\Pi_r = \frac{\Pi_{HTR-10}}{\Pi_{HTR-PM}}. \quad (37)$$

The ratio for the eight groups of similarity presented in the section above can be summarized as follows:

$$\left(\frac{Gr}{Re^2} \right)_r = \frac{G_{rm}}{G_{rp}} = \frac{(T_{sR} - T_{sS})_r H_{cav_r}}{V_{Re_r}^2}, \quad (38)$$

$$R_{a_r} = \frac{R_{am}}{R_{ap}} = (T_{sR} - T_{sS})_r H_{cav_r}^3, \quad (39)$$

$$P_{e_r} = \frac{P_{em}}{P_{ep}} = V_{Re_r} H_{cav_r}, \quad (40)$$

$$R_{i_r} = \frac{R_{im}}{R_{ip}} = \frac{Q_{0_r} H_{cav_r}}{V_{e_r}^3 A_{e_r}}, \quad (41)$$

$$S_{t_r} = \frac{S_{tm}}{S_{tp}} = V_{e_r}^{-0,2} D_r^{-1,2} H_{cav_r}, \quad (42)$$

$$N_{c_r} = \frac{N_{c_m}}{N_{c_p}} = \frac{A_{c_r} h_{cav_r}}{V_{e_r} A_{e_r}}, \quad (43)$$

$$N_{rad_r} = \frac{N_{rad_m}}{N_{rad_p}} = \frac{A_{rad_r} T_{in_r}^4}{Q_{0_r}}, \quad (44)$$

$$N_{T_r} = \frac{N_{T_m}}{N_{T_p}} = \frac{Q_{0_r}}{V_{e_r} A_{e_r} T_{in_r}}. \quad (45)$$

The only independent variables present in these similarity groups are D , V_e , T_{in} , and T_{out} , all of which belong to HTR-PM. The other variables are fixed according to the benchmark problem.

4. RESULTS

The HTR-10 data necessary for the similarity analysis were extracted from an atomic report by the International Atomic Energy Agency (IAEA) [3], whereas the HTR-PM data were extracted from Zheng [10]. All parameters used are summarized in Table 1:

Table 1: Parameters for the RCCS

Parameter	Symbol	HTR-10	HTR-PM	Ratio HTR-10/ HTR-PM
Heat removal by RCCS at steady-state conditions [kW]	Q_0	208.0	1107.0	0.1878
Cavity height [m]	H_{cav}	11.2	14.5	0.7724
Inner diameter of the standpipe [m]	D_i	0.032	0.032 ^a	1.000
Number of standpipes [-]	n	100	216	0.4629
Total cross flow area of the standpipes [m ²]	A_e	0.0804	0.1731	0.4629
Water velocity at the inlet of the standpipes [m/s]	V_e	0.0985	0.0985	1.000
Average temperature of the RPV wall [K]	T_{sS}	331.15	343.15	0.9650
Average temperature of the external wall of the standpipes [K]	T_{sR}	530.15	594.15	0.8923
Reference velocity in the air-cavity region [m/s]	V_{Re}	2.6588×10^{-6}	2.3699×10^{-6}	1.1218

Heat exchange coefficient for the air-cavity region [W/m ² K]	h_{cav}	2.3179	2.3490	0.9867
Total external area of the standpipe [m ²]	A_c	147.7805	413.2576	0.3575
Outer area of the standpipe facing the reactor [m ²]	A_{rad}	73.8902	206.6288	0.3575
Reference temperatures at the inlet of the standpipes [K]	T_{in}	323.15	338.15 ^b	0.9556
Reference temperatures at the outlet of the standpipes [K]	T_{out}	329.55	348.15 ^b	0.9465

a. Defined as that of HTR-10.

b. Value assumed based on the average temperature of the RCCS.

The water velocity at the inlet of the standpipes (V_e) for the HTR-PM is one of the parameters that were initially assumed to be equal to that of the HTR-10, and a sensibility analysis of the similarity of this parameter was conducted, i.e., assuming the values according to Table 2 below:

Table 2: Change of the water velocity at the inlet of the standpipes (V_e) for the HTR-PM

Change	V_e (m/s)	\dot{m}_e (kg/s) ^a
1	0.0585	10
2	0.0877	15
3	0.1170	20
4	0.1462	25
5	0.1755	30

a. mass flow rate at the inlet of the standpipes

The diameter of the standpipe of the HTR-PM was assumed to be the same as that of the HTR-10, and the water temperature at the inlet of the standpipes for the HTR-PM was fixed at 65°C. Thus, the only parameter not fixed was the water velocity at the inlet of the standpipes (V_e) of the HTR-PM. The results of these parameters in the eight similarity groups are summarized in Tables 3 and 4 below:

Table 3: Ratio of the similarity groups for the five changes in V_e of the HTR-PM

Change in V_e	$\left(\frac{Gr}{Re^2}\right)_{\text{For HTR-10}}$	$\left(\frac{Gr}{Re^2}\right)_{\text{For HTR-PM}}$	$\left(\frac{Gr}{Re^2}\right)_r$	$R_a_{\text{For HTR-10}}$	$R_a_{\text{For HTR-PM}}$	R_{a_r}
1 - 5	7.18×10^{12}	1.36×10^{13}	5.30×10^{-1}	5.10×10^{12}	9.46×10^{12}	5.39×10^{-1}

Table 4: Ratio of the similarity groups for the five changes in V_e of the HTR-PM

Change in V_e	P_{e_r}	R_{i_r}	S_{t_r}	N_{c_r}	N_{rad_r}	N_{T_r}
1	1.02	1.74×10^{-1}	3.93×10^{-1}	4.52×10^{-1}	1.59	2.52×10^{-1}
2	1.02	3.92×10^{-1}	5.89×10^{-1}	6.79×10^{-1}	1.59	3.78×10^{-1}
3	1.02	6.97×10^{-1}	7.85×10^{-1}	9.05×10^{-1}	1.59	5.04×10^{-1}
4	1.02	1.09	9.81×10^{-1}	1.13	1.59	6.30×10^{-1}
5	1.02	1.57	1.18	1.36	1.59	7.56×10^{-1}

The value of Gr/Re^2 for both the HTR-10 and HTR-PM presents a high order of magnitude, indicating a regime of natural air circulation within the cavity for both projects. The buoyancy forces dominate over the inertia forces for both reactors, and the ratio of the Gr/Re^2 value of the model to that of the prototype indicates that the HTR-10 presents a higher reference velocity than that of the HTR-PM. The Rayleigh number presents the same order of magnitude for both projects, and the ratios for both Gr/Re^2 and the value of Ra present approximately the same ratio, indicating that the flow conditions in the reactor cavities are similar.

The Richardson number represents the ratio of the buoyancy force to inertia force in the water flow analysis of the RCCS standpipes, and the ratio R_{i_r} depends on the water velocity at the inlet of the standpipes, presenting a ratio approximately equal to unity, where the value V_e is equal to 0.146 m/s (change 4), which represents a mass flow rate equal to 25 kg/s.

The Stanton number ratios present the same order of magnitude for all variations of V_e , indicating that the proportion of transferred heat in the standpipes is reasonable. For variation 4 of V_e , the St number indicates that the heat transfer capacity through the conduction of the HTR-PM is greater than that of the HTR-10. The number of standpipes in the HTR-PM is reasonably higher than that in the HTR-10 because of the need for a greater heat removal capacity of the cavity.

The value of N_{c_r} increases with the increase in the volumetric flow of the standpipes because it represents the relation between the heat transferred from the RPV to the standpipes through convection and the total amount of heat transferred. In variation 4 of V_e , the value of N_{c_r} is approximately equal to 1, indicating a similar convection heat transfer capacity. The value of N_{rad} represents the ratio of the heat transferred from the RPV to the standpipes through radiation and the total amount of heat transferred. The value of N_{rad} in variation 4 of V_e indicates that the radiation heat transfer of the HTR-10 is greater than that of the HTR-PM.

3. CONCLUSIONS

The HTR-10 is a proof-of-concept reactor for the HTR-PM with a thermal power of 250 MW, which requires a higher system capacity DHRS. A scale analysis of the reactor cavity cooling system between the reactors for the benchmark problem of a depressurized loss of forced cooling showed a similarity between the two projects, in terms of the simplification adopted in the

present work. The small differences in the numbers of certain groups of similarity indicate a small distortion between the physical phenomena occurring between the reactors, which can be justified owing to the differences between the reactors as well as the assumption of certain independent variables for the HTR-PM, such as the supposition of standpipes of the same diameter and the thickness between projects, along with the water temperature at the inlet of the standpipes of the HTR-PM.

ACKNOWLEDGMENTS

We thank the Conselho Nacional de Desenvolvimento Científico e Tecnológico (CNPq), the Coordenação de Aperfeiçoamento de Pessoal de Nível Superior (CAPES) and the Instituto Nacional de Ciência e Tecnologia de Reatores Nucleares Inovadores (INCT de Reatores Nucleares Inovadores) for giving us the financing and necessary support for the study.

REFERENCES

1. I. A. E. Agency, *Evaluation of high temperature gas cooled reactor performance: Benchmark analysis related to the PBMR-400, PBMM, GT-MHR, HTR-10 and the ASTRA critical facility (IAEA-TECDOC-1694)*, (2013).
2. I. A. E. Agency, *Decay heat removal and heat transfer under normal and accident conditions in gas cooled reactors (IAEA-TECDOC-757)*, no. July, (1992).
3. I. A. E. Agency, *Heat transport and afterheat removal for gas cooled reactors under accident conditions (IAEA-TECDOC-1163)*, IAEA, Vienna, (2001).
4. U.S. DOE Nuclear Energy Research Advisory Committee and Generation IV International Forum, *Technology Roadmap Update for Generation IV Nuclear Energy Systems*, (2014).
5. Y. Xu, S. Hu, F. Li, and S. Yu, "High temperature reactor development in China," *Proceeding of Progress in Nuclear Energy*, 260–270, (2005), **vol. 47**, no. 1–4, pp. 260–270.
6. Z. Zhang *et al.*, "The Shandong Shidao Bay 200 MWe High-Temperature Gas-Cooled Reactor Pebble-Bed Module (HTR-PM) Demonstration Power Plant: An Engineering and Technological Innovation," *Engineering*, **vol. 2**, no. 1, pp. 112–118, (2016).
7. Z. Zhang and Y. Sun, "Economic potential of modular reactor nuclear power plants based on the Chinese HTR-PM project," *Nuclear Engineering and Design*, **vol. 237**, no. 23, pp. 2265–2274, (2007).
8. Z. Zhang, Z. Wu, Y. Sun, and F. Li, "Design aspects of the Chinese modular high-temperature gas-cooled reactor HTR-PM," *Nuclear Engineering and Design*, **vol. 236**, no. 5–6, pp. 485–490, (2006).
9. Z. Zhang *et al.*, "Current status and technical description of Chinese 2 x 250 MWth HTR-PM demonstration plant," *Nuclear Engineering and Design*, **vol. 239**, no. 7, pp. 1212–1219, (2009).
10. Y. Zheng, L. Shi, and Y. Dong, "Thermohydraulic transient studies of the Chinese 200 MWe HTR-PM for loss of forced cooling accidents," *Annals of Nuclear Energy*, **vol. 36**, no. 6, pp. 742–751, (2009).